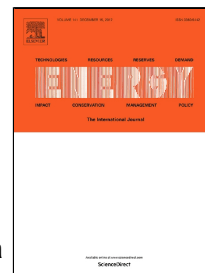# Accepted Manuscript

Deuterium Isotope Separation by Combined Electrolysis Fuel Cell

Ryota Ogawa, Risako Tanii, Richard Dawson, Hisayoshi Matsushima, Mikito Ueda

Please cite this article as: Ryota Ogawa, Risako Tanii, Richard Dawson, Hisayoshi Matsushima, Mikito Ueda, Deuterium Isotope Separation by Combined Electrolysis Fuel Cell, *Energy* (2018), doi: 10.1016/j.energy.2018.02.014

Deuterium Isotope Separation
by Combined Electrolysis Fuel Cell

Ryota Ogawa[1], Risako Tanii[1], Richard Dawson[2], Hisayoshi Matsushima[1*]
and Mikito Ueda[1]

[1]Faculty of Engineering, Hokkaido University,
Kita 13 Nishi 8, Sapporo, Hokkaido 060-8628, Japan.
[2] Faculty of Engineering, Lancaster University,
Gillow Avenue, Lancaster LA1 4YW, UK.
[*]Corresponding Author: matsushima@eng.hokudai.ac.jp
Tel. & Fax +81-11-7066352

Abstract

The framework about combined electrolysis fuel cell (CEFC) was reported previously [H. Matsushima et al., *Energy*, 2005; 30; 2413]. The purpose of the present study focused on measuring the separation factor and the energy reduction by assembling CEFC system. The separation of deuterium was studied with a 1-M KOH electrolyte containing 10 at% deuterium. Polarization plots of alkaline water electrolysis (AWE) revealed relationships between the catalytic activity of the hydrogen evolution reaction and the deuterium separation factor. The power loss was mainly attributed to gas bubble evolution. For polymer electrolyte fuel cells (PEFCs) with a Pt catalyst, approximately 21% of the electrical energy could be recovered by reusing hydrogen gas produced by the AWE. Furthermore, the PEFC could efficiently dilute protium in the gas phase, resulting in a high separation factor of 30.2 for the CEFC.

Keywords: Void fraction; Electrolysis; Energy Efficiency; Fuel Cell

1. **Introduction**

Hydrogen is one of the most abundant elements on the earth and has three principal isotopes. It exists in nature as two main isotopes, protium (H) and deuterium (D), although deuterium makes up only 150 ppm of naturally occurring hydrogen. Deuterium and tritium (T) are important materials in the field of energy. In heavy-water reactor designs, deuterium is used as a moderator for slow neutrons in fission reactions. Tritium is produced as a by-product of this process. Nuclear fusion reactors are expected to become part of future power systems and deuterium and tritium are used for the D-T fusion reaction, which can release large amounts of energy [1]. However, tritium contamination of water represents a hazard to human health and the environment. Hence, decontamination technologies are required to enable efficient separation and storage of tritium [2, 3].

The separation of hydrogen isotopes is difficult because their chemical properties are very similar. Studies of this issue date back to the 1930s [4, 5] and continue today. The major hydrogen separation processes used industrially [6], include: distillation, which operates based on the difference in the equilibrium vapor pressure of the isotopes [7]; chemical exchange, which is based on isotope exchange reactions on catalysts [8]; and water electrolysis, which exploits differences in the kinetics of the hydrogen evolution reaction (HER) between different isotopes [9-13]. Water electrolysis is the most effective separation method and the separation factor has been reported to be in the range of 5–8 for protium and deuterium [11, 13]. Although water electrolysis has advantages in terms of its high separation factor, it has a critical drawback in that it requires an enormous amount of electrical energy. Therefore, combined electrolysis catalytic exchange (CECE) is commonly used. In CECE, hydrogen generated from electrolysis is passed through a Pt catalysis column [14]. Hydrogen gas containing heavier isotopes is preferentially exchanged to the liquid phase (*ex.* $HD_{gas} + H_2O_{liq} \rightarrow HDO_{liq} + H_{2gas}$) at the Pt catalyst. Owing to the spontaneous exchange reaction, CECE can enrich isotopes in the liquid phase without any additional energy input. However, the high energy consumption remains problematic for water electrolysis and practical constraints such as the need for a long catalyst column limit throughput.

To address these issues, we have proposed new a hydrogen separation system, named *CEFC* [15]. In this system, hydrogen and oxygen gases from electrolysis are used for electricity generation in a fuel cell. This reaction enables a portion of the energy used for electrolysis to be offset so that the external electrical power requirement is greatly reduced.

The essential problems of energy consumption are attributed to water electrolysis in both CEFC and CECE. Many fundamental studies of HER kinetics have been conducted [16-20]; however, practical engineering approaches have been discussed less frequently. Formation of gas bubbles is one of the main problems for operating water electrolysis at high current density [21-25]. The bubbles disperse into the electrolyte and shield the electrode to markedly decrease the energy efficiency. Vogt and coworkers have summarized the effects of bubbles during water electrolysis [26, 27].

To consider the full advantages of a CEFC system, it is necessary to investigate not only energy consumption but also the synergetic effects of additional separation in the fuel cell. It has been reported that the kinetic isotope effect of the hydrogen oxidation reaction is also been observed in PEFCs [28-31]. Hence, CEFCs have the potential to separate hydrogen isotopes more efficiently and cheaply than CECEs. However, a combined system, in which AWE provides a fuel source, has not yet been reported. In the present study, after the CEFC was fabricated by the combination of AWE and PEFC, we investigated the energy efficiency and deuterium separation ability of the system.

2. Experimental

2.1 AWE operation

AWE was performed in a small scale electrolyzer (Y5390, Pelmelec Electrode Ltd., Japan), as shown in Fig. 1. A pure Ni electrode was used as the anode. Three types of electrodes (Pt, Ni, and $NiCo_2O_4$) were used as the cathode. Both the anode and cathode electrodes were mesh-shaped and their apparent surface area was 35 cm^2. The electrodes were sandwiched by a thin porous membrane filter to separate the anolyte and catholyte. Two mercury oxide electrodes (Hg/HgO) were used for reference electrodes and were connected near the anode and cathode surface by a Lugging capillary. Potassium hydroxide (1 M KOH) was used as the electrolyte. The deuterium concentration of the solution was adjusted to 10 at% by addition of heavy water (99.9% D_2O, Sigma-Aldrich, Japan). The AWE was operated at a constant current density at 298 K. The transient behavior of the electrolysis voltage and the anode / cathode potential were simultaneously recorded by a digital logger (Midi Logger GL220, Graphtech, Japan).

The deuterium separation factor of AWE was measured by a quadrupole mass spectrometer, Q-mass (Qulee-HGM 202, Ulvac Corp., Japan). The hydrogen gas generated from the cathode directly flowed to the mass spectrometer through Line A

3

(Fig. 2). The flow rate was controlled with a needle valve so that the total pressure in
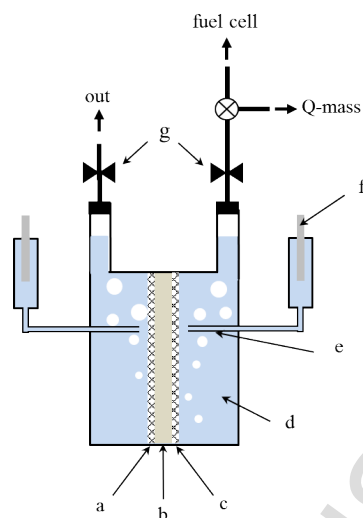

Fig. 1 Schematic illustration of alkaline water electrolysis cell. (a) Anode, (b) membrane, (c) cathode, (d) electrolyte, (e) Luggin capillary, (f) reference electrode, (g) valve.

the mass spectrometer chamber was constant. The ion currents of the three gas species, with masses m = 2, 3, and 4 representing H_2, HD, and D_2, respectively, were monitored in-situ. Measurements were performed for at least 3 h to ensure steady state conditions.

2.2 PEFC operation

The PEFC set up has been described in our previous paper [29], therefore, only the main points are mentioned here. Japan Automobile Research Institute (JARI) standard cell (FC Development Corp., Japan) was used. The membrane electrode assembly (50 × 50 mm^2) was composed of a Nafion electrolyte (NRE-212) and two catalytic layers loaded with platinum catalyst (Pt 0.50 mg cm^{-2}). The cell was operated at 298 K. The cell performance was investigated with the output current controlled by an adjustable resistor (PLZ164WA, Kikusui Electronics Corp., Japan). Hydrogen gas was supplied from the AWE. Electrolysis was performed at constant currents of 1, 3, and 5 A. Pure oxygen gas was supplied directly from a gas bottle.

The separation factor of the PEFC was measured together with that of the AWE. The outlet gas from the anode was connected to the mass spectrometer through Line B (Fig. 2). By comparing the results from Line A and B, we discuss the separation factor of the PEFC and CEFC, respectively.
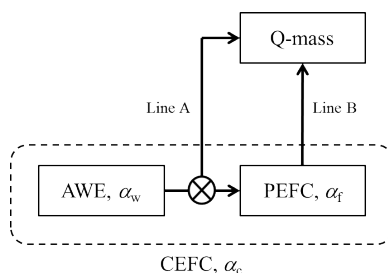
3 Results and discussion

4

3.1 AWE

Fig. 2 Schematic diagram of hydrogen gas line. Separation factor symbols α are noted for each device.

Water electrolysis plays important roles in both isotope separation and consumption of electrical energy in CEFCs. Typical cathode materials of AWEs are selected from precious and non-precious metals, while the anode is fixed as pure Ni. The electrolysis voltage V_W across the cathode and anode was recorded. Figure 3 shows the current/voltage plots. All cathode materials featured an onset voltage of approximately 1.6 V. The curves measured for the Pt and Ni electrode were similar. The Ni electrode was active for HER as expected from volcano plots [32]. Interestingly, V_w of $NiCo_2O_4$ was smaller than the cell voltages of other materials when electrolysis was operated at low current densities ($i < 60$ mA cm^{-2}). The low value suggested a high catalytic activity for HER.

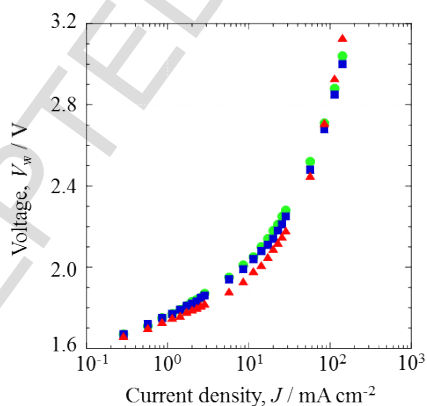Fig. 3 Current-voltage plots of AWE with various cathode electrodes at 298 K (Pt, ●; Ni, ■; $NiCo_2O_4$, ▲).

The I-V_w plots of all the cathode materials changed at $i > 10$ mA cm^{-2}. At this current density gas bubble evolution was confirmed and bubble formation increased the voltage markedly. Many fine bubbles of hydrogen (with diameters less than 1 mm) detached from the electrode and moved upward owing to natural macroscopic

5

convection [33]. The dispersed bubbles turned the appearance of the electrolyte milky and many bubbles were evolved at a high current density ($i > 80$ mA cm^{-2}). We did not recognize any influence of the cathode materials on the hydrogen evolution behavior in the present experiment. The oxygen bubbles coalesced with neighboring bubbles and grew in diameter to 2–3 mm. The bubble size showed no dependence on the electrolysis current. Some large bubbles detached and rose up while rolling on the electrode surface.
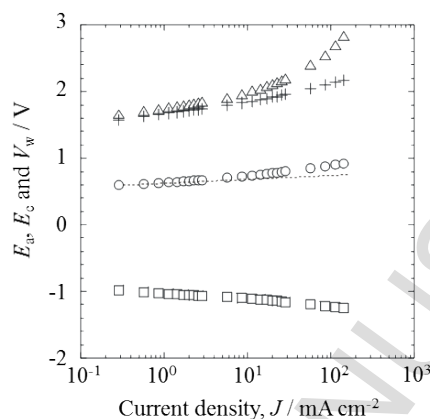

Fig. 4 Comparison of current-voltage (Vw, △), -Ni anode potential (Ea, ◯) and NiCo$_2$O$_4$ cathode potential (Ec, ▢) plots of AWE in 1 M KOH containing 10 at% deuterium at 298 K. Cross symbols indicate |Ea| + |Ec|.

The gas bubbles apparently depressed the electrolysis efficiency as the applied current was increased. Two reference electrodes were used at the cathode and anode to estimate the voltage drop (IR drop). Figure 4 shows current-potential plots for the NiCo$_2$O$_4$ cathode. The cathode potential E_c decreased with a Tafel slop of 0.13 V dec^{-1}. This value agrees well with that of other transition metal electrodes [34]. The linearity of E_c suggested that the reaction area remained unchanged. The hydrophobic effect likely induced hydrogen bubble to break off from the electrode surface. The anode potential E_a deviated from the broken line when oxygen bubbles were evolved at $i > 10$ mA cm^{-2}. This variation reached 0.18 V at 150 mA cm^{-2}. We previously measured the contact angle during electrolysis and found poor wettability [35]. Together with the present results, we confirmed that oxygen bubbles reduced the reaction area by adhering to and covering the Ni surface. At 150 mA cm^{-2} we estimated that the effective surface coverage decreased to approximately 30% of the actual surface area [36].

The electrolysis voltage was almost equal to the sum of $|E_a|$ and $|E_c|$, when few gas bubbles were evolved. Thus, the ohmic resistance of the thin electrolyte membrane could be ignored. However, the electrolysis voltage increased markedly at $i > 10$ mA cm^{-2}. The required overvoltage at 150 mA cm^{-2} was 0.84 V. This value was

6

equivalent to approximately 30% of the electric power consumption (compared with the sum of E_a and E_c, i.e., 2.8 V). This large energy loss was caused by the high void fraction, ε [37, 38]. Gas bubbles blocked the electrical pathway in the electrolyte and reduced the apparent electric conductivity. The value of ε was calculated by the Bruggeman equation,

$$\rho = \rho_0(1-\varepsilon)^{-3/2} , \qquad (1)$$

where ρ and ρ_0 are the resistivity values of the electrolyte with and without gas bubbles, respectively.

The voltage deviation of Fig. 4 was analyzed and the dependency of ε on the current density is shown in Fig. 5. The value of ε contains factors from both hydrogen and oxygen bubbles. The void remarkably increased with increasing current density ($i \geq 7$ mA cm^{-2}), and approached a value of 0.8 at high current density. We have previously reported on water electrolysis under microgravity conditions [35], where the absence of buoyancy resulted in a close-packed bubble layer. The ε value of the bubble layer was 0.75, which was similar to that of the present results. It is likely that only a small amount of electrolyte remained in the tiny gap between gas bubbles.
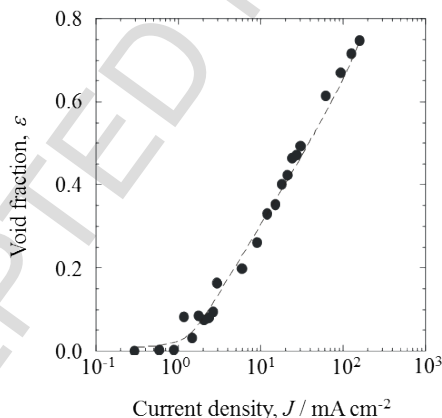

Fig. 5 Dependency of void fraction ε on electrolysis current density (referring to data in Fig. 3)

The ratio of protium and deuterium in the hydrogen gas was measured during electrolysis. The ion currents of mass number $m = 2$, 3, and 4 were monitored and assigned to H$_2$ ($m = 2$), HD ($m = 3$) and D$_2$ ($m = 4$), respectively [29]. The mass spectrometer data suggested that almost all the hydrogen gas containing D was evolved as HD molecules rather than as D$_2$ (Table 1). This phenomenon was confirmed for all the cathode materials tested. Here the deuterium separation factor α_w of the AWE is

defined by Eq.(2),

$$\alpha_w = ([H]/[D])_g/([H]/[D])_l, \qquad (2)$$

where [H] and [D] are the molar concentration of protium and deuterium, and the subscripts g and l indicate the gas and liquid phases of the electrolyte, respectively. The values of α_w are summarized in Table 2. The AWE contained a protium enriched gas phase, while deuterium was concentrated in the electrolyte. The effectiveness of the separation process was demonstrated over long term operation. The $NiCo_2O_4$ electrode gave the highest separation ($\alpha_w = 8.0$) of all three samples. The cobalt metal is active for reducing the oxides, especially the oxide layer weakly bonding with utmost metal surface. The bare metal surface is suitable for HER, which is explained by Rowland effect [13]. Thus, the present results suggested that, by lessening the overpotential of HER, light water was preferentially taken part in the reduction reaction, as shown in Fig. 3, the active electrode for HER gave better separation performance. This probably attributed to the highest separation factor of $NiCo_2O_4$.

Table 1 Ion current data of mass spectrometer measured during AWE operation with the use of several cathodes at 298 K (electrolysis current, 5 A; deuterium concentration, 10 at%).

Cathode $\diagdown$ m	2	3	4
Pt	9.2×10^{-9}	2.9×10^{-10}	4.0×10^{-12}
Ni	9.5×10^{-9}	2.9×10^{-10}	3.8×10^{-12}
$NiCo_2O_4$	7.3×10^{-9}	2.0×10^{-10}	2.7×10^{-12}

Unit : A

Table 2 Deuterium separation factor α_w of AWE at 298 K for various of cathode materials.

Cathode	Pt	Ni	$NiCo_2O_4$
α_w	6.9	7.2	8.0

3.2 CEFC

AWE occurred at the Ni cathode and the evolved hydrogen gas was directly supplied to the PEFC. The flow rate was controlled by the electrolysis current. The power current of the PEFC was adjusted from 0.0 to 4.0 A in 0.2 A increments, while the AWE was operated at 5 A. Figure 6 shows the fuel cell voltage V_f and the power P_f at various power currents. The open circuit voltage was approximately 1.0 V, which

8

was a reasonable value considering that pure oxygen gas was used. When the PEFC was initially operated at 0.2 A, the cell voltage dropped to 0.85 V because of the activation overvoltage. Subsequently, the voltage decreased linearly with increasing power current. This relationship was attributed mainly to the energy loss caused by the ohmic resistance of the PEFC. We could operate the PEFC at up to 4.0 A and obtained a maximum electric power of 2.8 W. However, this performance was poorer than that of previous reports [39]. The main reason for this difference can be explained by the low temperature of our experiments. Several undesirable factors such as the low conductivity of Nafion, flooding problems, and inactivation of the catalyst occur at low temperatures. However, it should be noted that the present power problem did not affect the deuterium separation in CEFC, as discussed later.
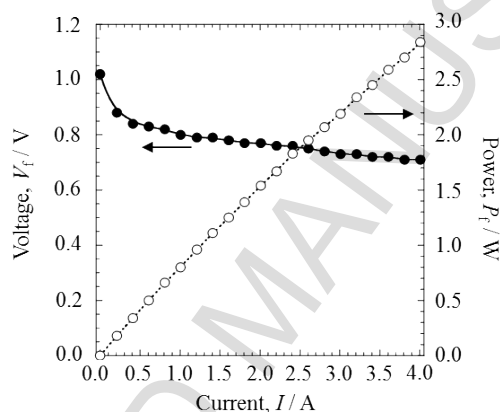

Fig. 6 Cell voltage (●) and power (○) plots of PEFC operated with hydrogen gas supplied from AWE in 1 M KOH containing 10 at% deuterium at 298 K.

The PEFC was continuously operated and the outlet gas line (Line B) was directly connected to the mass spectrometer, as shown in Fig. 2. The mass components of the outlet gas from the PEFC anode were analyzed. The power current was increased after we confirmed steady state data from the mass spectrometer. Figure 7 shows the ion currents of $m = 2, 3, 4$. The open circuit potential (OCP) state was maintained for the first hour of operation. The gas components without any electrochemical reactions were also investigated. In our previous research, we used a cylinder of D_2 gas and reported that D_2 molecules changed into HD through an isotope exchange reaction ($H_2 + D_2 \rightarrow$ 2HD) [28]. The present data suggested that the exchange reaction did not take place, because hydrogen gas from the AWE had already been produced as HD molecular (Table 1).
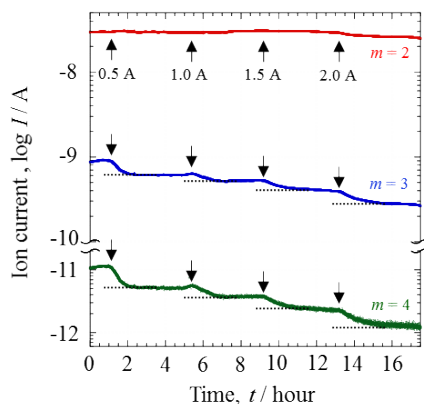
9

Fig. 7 Transient behavior of mass spectra for mass numbers, $m = 2$ (red line), 3 (blue line) and 4 (green line) during PEFC operation with hydrogen gas supplied from the AWE at 298 K. Arrows indicate a change of the power current of the PEFC.

When the PEFC generated power, the ratios of both HD:H_2 and D_2:H_2 gases decreased, and the decrease depended on the power current. Thus, the gases containing deuterium were preferentially consumed. This might be attributed to the kinetic difference of the electrochemical oxidation reaction. Some researchers have reported that the Tafel slope of deuterium oxidation reactions is a few mV smaller than that of protium [19] and that the exchange current also differs [29]. It should be emphasized that the reduction ratio of HD was smaller than that of D_2. For example, the ionic currents of HD and D_2 decreased by approximately 70% and 90% compared with the initial value, respectively. Thus, the effects on molecules of heavier mass were more pronounced, indicating an isotope effect.

The deuterium separation factor α_f of the PEFC was investigated at several electrolysis currents. We monitored the mass spectrometer data at the OCP and confirmed that the deuterium concentration remained almost constant regardless of the electrolysis current. The value of α_f was calculated as follows,

$$\alpha_f = ([H]/[D])_{after} / ([H]/[D])_{before} , \qquad (3)$$

where the subscripts 'after' and 'before' indicate the ratio observed *after* and *before* power generation by PEFC. Table 3 shows α_f and molar concentration of protium and deuterium calculated by the ion current in Fig.7. To consider the energy efficiency of the PEFC, the fuel utilization U_f is defined as follows,

10

$$U_f = V_f / V_w , \tag{4}$$

Table 3   Deuterium separation factor a_f of PEFC and molar concentration of protium and deuterium measured after and before power generation operated at several power currents at 298 K.

Power current / A	0	0.5	1.0	1.5	2.0
α_f	-	1.5	1.8	2.3	2.9
H / %	98.47	98.97	99.14	99.32	99.47
D / %	1.53	1.03	0.86	0.68	0.53

where V_f is the gas volume consumed in the PEFC and V_w is the gas volume supplied from the AWE. The value of α_f was plotted against U_f and showed a linear relationship, as shown in Fig. 8.
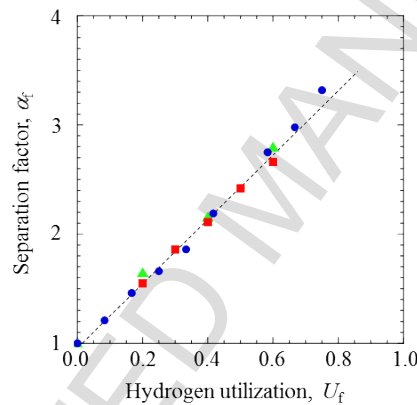

Fig. 8 Dependence of the deuterium separation factor α_f on the hydrogen utilization U_f of the PEFC during AWE operation at various electrolysis currents (1 A, ▲; 3 A, ●; and 5 A, ■).

When the value of U_f was low, a large amount of hydrogen gas passed through the gas diffusion layer (GDL) without making any contribution to the oxidation reaction. Thus, the ratio of the unreacted gas decreased with increasing U_f, which likely contributed to the observed linearity.

The AWE was performed at a constant current of 3 A when the separation of CEFC was studied. As for the PEFC experiment, we changed the power current from 0 to 2.25 A and monitored the deuterium concentration from Line B (Fig. 2). The separation factor α_c of the CEFC was defined as follows,

$$\alpha_c = ([H]/[D])_{after}/([H]/[D])_l. \tag{5}$$

11

The power consumption of CEFC P_c was calculated as follows,

$$P_c = P_w - P_f, \qquad (6)$$

where P_w is the electric consumption by the AWE. Figure 9 shows the relationship between α_c and P_c. Table 4 summarizes P_c, α_c and molar concentration of protium and deuterium at several power currents of fuel cell. Notably, when the PEFC was not operated (red plot), $\alpha_c = 9.4$ did not coincide with $\alpha_w = 7.2$, as shown in Table 2. The small improvement indicated that a small amount of the dissociated D_2 could diffuse and combine with water at the cathode side as previously reported [28]. The exchange reaction occurs even at OCP between dissociated ions (H^+ or D^+) in Nafion membrane and vapor (H_2O) in cathode gas. Therefore, slight deuterium separation was observed.

Table 4 P_c, a_c and molar concentration of protium and deuterium measured in CEFC system.

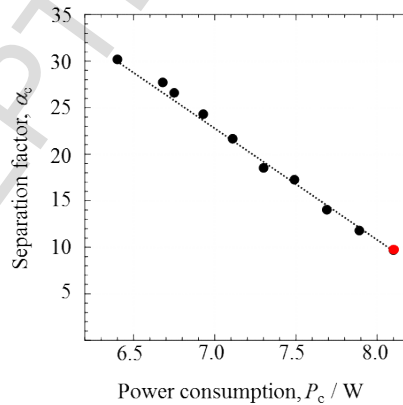| Power current / A	0	0.25	0.50	0.75	1.00	1.25	1.50	1.75	2.00	2.25
P_c / W	8.1	7.9	7.7	7.5	7.3	7.11	6.9	6.8	6.7	6.4
α_c / W	9.7	11.8	14.0	17.3	18.5	21.7	24.3	26.6	27.7	30.2
H / %	98.87	99.07	99.21	99.36	99.40	99.49	99.54	99.58	99.60	99.63
D / %	1.13	0.93	0.79	0.64	0.60	0.51	0.46	0.42	0.40	0.37

Fig. 9 Relationship between the deuterium separation factor α_c and total power consumption of CEFC.

In terms of energy consumption, P_c was reduced with increasing P_f under constant voltage AWE. A maximum electrical energy recovery of 21% was achieved at $U_f = 0.75$ in the present experiment. The main factors contributing to the energy loss

were the activation overpotential at the PEFC and the evolution of bubbles from AWE, as discussed above. The separation factor increased markedly with decreasing P_c. This was a desirable result for applications to separation. The value jumped to $\alpha_c = 30.2$ at $P_c = 6.4$ W. The value of α_c was almost equal to the product of $\alpha_w \times \alpha_f$. Thus, the CEFC could take advantage of the multiplier effect for isotope separation. Moreover, we expected that our CEFC system could separate isotopes, using even less electrical energy when operated at high temperature (ca. 353 K).

4. Conclusion

The CEFC system presented here clearly showed effective deuterium separation through a combination of AWE and a PEFC. Our findings correlated well with the expected kinetic isotope effects of these electrochemical reactions. More detailed investigations of AWE, allowed us to identify an active electrode material for HER, namely $NiCo_2O_4$, which showed an α_w of 8.0 in 1 M KOH containing 10 at% deuterium. A large portion of the electrolysis power was consumed through the evolution of bubbles. On the basis of studies of the ohmic resistance during electrolysis we attributed these energy losses to the high void fraction of $\varepsilon \approx 0.8$ and the low surface coverage of $\theta \approx 0.3$. The mass spectra measured from the PEFC showed that the value of α_f depended on hydrogen utilization, irrespective of the AWE conditions. The application of the PEFC enabled recovery of approximately 21% of the electrical energy and achieved a high separation factor of $\alpha_c = 30.2$ at 298 K. These data indicate that dual isotope separation by the combination of electrolysis and a fuel cell, is suitable for applications to industrial separation processes. It can be used for making high purity hydrogen isotopes used in not only the field of energy but also organic chemistry, biochemistry, pharmaceutical research. The characteristics of CEFC system reducing heavy hydrogen isotopes concentration in the gas are suitable for the wastewater treatment of the reactor and recovering energy system [40]. Furthermore, it is also helpful for demonstration of the industry developing for hydrogen energy society.

Figure Captions

Table 1

Ion current data of mass spectrometer measured during AWE operation with the use of several cathodes at 298 K (electrolysis current, 5 A; deuterium concentration, 10 at%).

Table 2

Deuterium separation factor α_w of AWE at 298 K for various of cathode materials.

Table 3

Deuterium separation factor α_f of PEFC and molar concentration of protium and deuterium measured after and before power generation operated at several power currents at 298 K.

Table 4

P_c, α_c and molar concentration of protium and deuterium measured in CEFC system

Figure 1

Schematic illustration of alkaline water electrolysis cell. (a) Anode, (b) membrane, (c) cathode, (d) electrolyte, (e) Luggin capillary, (f) reference electrode, (g) valve.

Figure 2

Schematic diagram of hydrogen gas line. Separation factor symbols α are noted for each device.

Figure 3

Current-voltage plots of AWE with various cathode electrodes at 298 K (Pt, ●; Ni, ■; $NiCo_2O_4$, ▲).

Figure 4

Comparison of current-voltage (V_w, △), -Ni anode potential (E_a, ○) and $NiCo_2O_4$ cathode potential (E_c, □) plots of AWE in 1 M KOH containing 10 at% deuterium at 298 K. Cross symbols indicate $|E_a| + |E_c|$.

Figure 5

Dependency of void fraction ε on electrolysis current density (referring to data in Fig.

14

3).

Figure 6
Cell voltage (●) and power (○) plots of PEFC operated with hydrogen gas supplied from AWE in 1 M KOH containing 10 at% deuterium at 298 K.

Figure 7
Transient behavior of mass spectra for mass numbers, $m = 2$ (red line), 3 (blue line) and 4 (green line) during PEFC operation with hydrogen gas supplied from the AWE at 298 K. Arrows indicate a change of the power current of the PEFC.

Figure 8
Dependence of the deuterium separation factor α_f on the hydrogen utilization U_f of the PEFC during AWE operation at various electrolysis currents (1 A, ▲; 3 A, ●; and 5 A, ■).

Figure 9
Relationship between the deuterium separation factor α_c and total power consumption of CEFC.

References

[1]   Rebut PH, *Energy*, 1993; 18:1023-1031.

[2]   Morgenstern U, Taylor CB, *Isot. Environ. Health Stud.*, 2009; 45: 96-117.

[3]   Vasyanina TV, Alekseev IA, Bondarenko SD, Fedorchenko OA, Konoplev KA, Arkhipov EA, Uborsky VV, *Fusion Eng. Des.*, 2008; 83: 1451-1454.

[4]   Washburn EW, Urey HC, *Proc. Natl. Acad. Sci. U. S. A.*, 1932; 18: 496-498.

[5]   Topley B, Eyring H, *J. Chem. Phys.*, 1934; 2: 217-230.

[6]   Miller MM, *Energy*, 1984; 9: 829-846.

[7]   Fukada S, *J. Nucl. Sci. Technol.*, 2004; 41: 619-623.

[8]   Sugiyama T, Takada A, Morita Y, Kotoh K, Munakata K, Taguchi A, Kawano T, Tanaka M, Akata N, *Fusion Eng. Des.*, 2015; 98-99:1876-1879.

[9]   Greenway SD, Fox EB, Ekechukwu AA, *Int. J. Hydro. Energy*, 2009; 34: 6603-6608.

[10]   Ogata Y, Sakuma Y, Ohtani N, Kotaka M, *Fusion Sci. Technol.*, 2005; 48: 136-139.

[11]   Matsushima H, Nohira T, Ito Y, *Electrochim. Acta*, 2004; 49: 4181-4187.

[12]   Aprea JL, *Int. J. Hydro. Energy*, 2002; 27: 741-752.

[13]   Stojic DLJ, Miljanic SS, Grozdic TD, Bibic NM, Jaksic MM, *Int. J. Hydro. Energy*, 1991; 16: 469-476.

[14]   Paek S, Ahn DH, Choi HJ, Kim KR, Lee M, Yim SP, Chung H, Song KM, Sohn SH, *Fusion Eng. Des.*, 2007; 82: 2252-2258.

[15]   Matsushima H, Nohira T, Kitabata T, Ito Y, *Energy*, 2005; 30:2413-2423.

[16]   Tse ECM, Hoang TTH, Varnell JA, Gewirth AA, *ACS Catal.*, 2016; 6: 5706-5714.

[17]   Krishtalik LI; *Electrochim. Acta*, 2001; 46: 2949-2960.

[18]   Kuhn AT, Byrne M, *Electrochim. Acta*, 1971; 16: 391-399.

[19]   Bockris JO, Srinivasan S, *J. Electrochem. Soc.*, 1964; 111: 853-858.

[20]   Conway BE, *Proc. R. Soc. A Math. Phys. Eng. Sci.*, 1958; 247: 400-419.

[21]   Zhang DK, Zeng K, *Ind. Eng. Chem. Res.*, 2012; 51: 13825-13832.

[22]   Iida T, Matsushima H, Fukunaka Y, *J. Electrochem. Soc.*, 2007; 154: E112-E115.

[23]   Philippe M, Jerome H, Sebastien B, Gerard P, *Electrochim. Acta*, 2005; 51: 1140-1156.

[24]   Mat MD, Aldas K, Ilegbusi OJ, *Int. J. Hydro. Energy*, 2004; 29: 1015-1023.

[25]   Hine F, Murakami K, *J. Electrochem. Soc.*, 1980; 127: 292-297.

[26] Vogt H, *Electrochim. Acta*, 2011; 56: 1409-1416.

[27] Vogt H, Balzer RJ, *Electrochim. Acta*, 2005; 50: 2073-2079.

[28] Matsushima H, Ogawa R, Shibuya S, Ueda M, *Materials*, 2017; 10: 303

[29] Shibuya S, Matsushima H, Ueda M, *J. Electrochem. Soc.*, 2016; 163: F704-F707.

[30] Ogawa R, Matsushima H, Ueda M, *Electrochem. Commun.*, 2016; 70: 5-7.

[31] Yanase S, Oi T, *Zeitschrift Für Naturforsch. A.*, 2015; 70: 429-435.

[32] Conway BE, Jerkiewicz G, *Electrochim. Acta*, 2000; 45: 4075-4083.

[33] Vogt H, *Electrochim. Acta*, 1993; 38: 1421-1426.

[34] Hall DS, Bock C, MacDougall BR, *J. Electrochem. Soc.*, 2013; 160: F235-F243.

[35] Matsushima H, Nishida T, Konishi Y, Fukunaka Y, Ito Y, Kuribayashi K, *Electrochim. Acta*, 2003; 48: 4119-4125.

[36] Vogt H, *Electrochim. Acta*, 2017; 235: 495-499.

[37] El-Askary WA, Sakr IM, Ibrahim KA, Balabel A, *Energy*, 2015; 90: 722-737.

[38] Mandin P, Derhoumi Z, Roustan H, Rolf W, *Electrochim. Acta*, 2014; 128: 248-258.

[39] Hashimasa Y, Matsuda Y, Shimizu T, *Electrochim. Acta*, 2015; 179: 119-125.

[40] Børset TM, Wilhelmsen Ø, Kjelstrup S, Burheim OS, *Energy*, 2017; 118: 865-875.

Highlights

•Water electrolysis and polymer electrolyte fuel cell can separate hydrogen isotopes

•The fuel cell reduced electric power consumption by approximately 21%

•High separation factor was achieved by water electrolysis combined with a fuel cell